Magnetic depth profiles from resonant soft x-ray scattering: Application to Dy thin films

H. Ott,[a),b)] C. Schüβler-Langeheine,[a)] E. Schierle, G. Kaindl, and E. Weschke
Institut für Experimentalphysik, Freie Universität Berlin, 14195 Berlin, Germany

(Received 20 December 2005; accepted 27 April 2006; published online 24 May 2006)

We employ the strong variation of the photon penetration depth across an electronic resonance in soft x-ray scattering for a depth resolved study of an antiferromagnetic (AFM) thin film. We directly observed the development of the helical AFM structure in thin Dy(001) films on W(110) across the temperature-induced phase transition from ferromagnetic to helical AFM order. © *2006 American Institute of Physics*. [DOI: 10.1063/1.2206699]

The knowledge of the magnetic depth profile at interfaces is crucial for an understanding of the properties of systems based on magnetic thin films, e.g., in magnetic devices such as magnetic sensors and storage media. As a consequence, there have been quite a few efforts to obtain spatial-resolved information about magnetic structures and domains. A lateral resolution can be achieved by a variety of microscopy techniques such as scanning tunneling microscopy (STM), magnetic force microscopy (MFM), Lorentz microscopy, and spin-polarized low energy electron microscopy (SPLEEM). While these techniques are sensitive to ferromagnetic (FM) domains, antiferromagnetic (AFM) domains have been studied by x-ray diffraction using a focusing optics to get lateral resolution.[1] It is more demanding to obtain depth-resolved information on the magnetic structure, e.g., by spin-polarized neutron reflectivity.[2,3] Such methods do not intrinsically limit the probing depth but are based on detailed model calculations for extraction of magnetization profiles. In-plane information on the magnetic structure with a certain depth resolution can be derived from birefringent in-plane Bragg diffraction of evanescent neutron states below the angle of total reflection.[4–6] Generally the limits of surface-sensitive neutron scattering are posed by the low scattering intensity and the moderate depth sensitivity.[5] For x rays the penetration depth varies with photon energy, in particular, near absorption thresholds. While for resonances in the conventional x-ray range this is a rather weak effect, the change of the photon mean free path at resonances in the soft x-ray range, e.g., at the lanthanide $M_{4,5}$ and transition-metal $L_{2,3}$ thresholds, is sufficiently huge to exploit this effect to vary the probing depth.

Here, we report the application of this effect for a direct observation of magnetic depth profiles in AFM thin films. We demonstrate this technique for thin Dy films grown on W(110). Bulk Dy metal is FM below T_C=89 K and AFM between T_C and T_N=179 K with a helical AFM structure propagating along the crystallographic c axis leading to a superstructure peak in the magnetic diffraction signal, which is offset by $\pm(00\tau)$, $\tau\approx0.185$, from the fundamental Bragg peaks. The transition between both magnetic phases has a hysteretic and discontinuous first-order character not only in bulk samples but also in various thin-film and multilayer systems.[7–9] In contrast to that, the system studied here shows a gradual FM-AFM transition involving temperature-dependent growth of the antiferromagnetic domain in the presence of still ferromagnetically ordered parts of the film.

Reference scattering experiments at the Dy L_3 absorption threshold were performed at ID 10A of the ESRF in Grenoble.[10] The soft x-ray data were recorded at the U49/1 beam line of the Berliner Elektronenspeicherring für Synchrotronstrahlung (BESSY) in Berlin, using an ultrahigh-vacuum ($\Theta/2\Theta$) diffractometer. High quality Dy films were grown *in situ* in UHV under identical conditions in the corresponding setups. To record the temperature-dependent data the sample temperature was cycled several times from well above T_N down to 40 K and back in steps of 1–20 K with a waiting time per data point of at least 10 min.

The gradual character of the phase transition can be already seen from the resonant diffraction data in the conventional x-ray range. Figure 1(a) displays the intensity of the (002-τ) magnetic satellite as recorded at the Dy L_3 threshold ($h\nu$=7780 eV). The satellite intensity is proportional to the squared AFM order parameter.[11,12] At this resonance the x-ray probing depth of ≈9 μm is much larger than the film thickness, such that all layers of the film contribute about equally to the magnetic signal. When cooling below ≈70 K (open symbols) the (002-τ) satellite disappears in a narrow

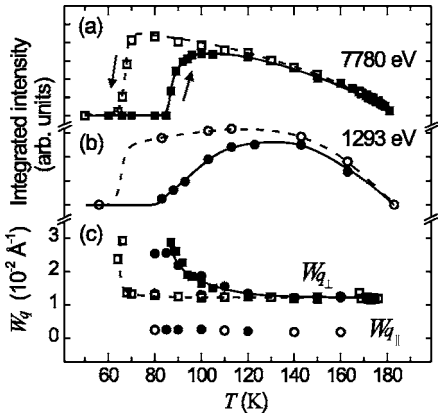

FIG. 1. Magnetic diffraction data characterizing the FM/helical AFM phase transition in 180-ML Dy/W(110) upon cooling down (open symbols) and warming up (filled symbols); lines serve as guides for the eye. (a) Integrated intensities of (002-τ) at the L_3 resonance (7780 eV). (b) Analogous data from (00τ) recorded at the M_5 resonance. (c) Widths of magnetic peaks in the directions parallel ($W_{q_\parallel}$) and perpendicular ($W_{q_\perp}$) to the film plane recorded at 7780 eV (squares) and at 1305 eV (circles).

a)Present address: II. Physikalisches Institut, Universität zu Köln, Zülpicher Str. 77, D-50937 Köln, Germany.
b)Electronic mail: ott@ph2.uni-koeln.de

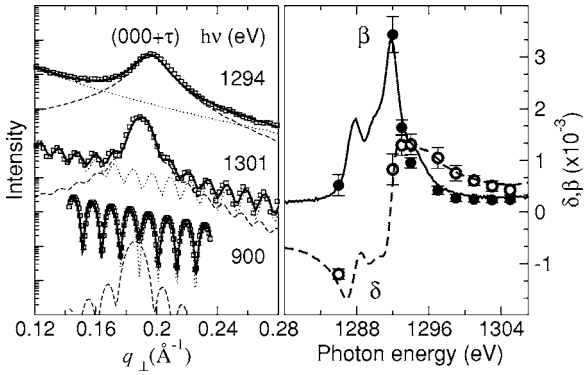

FIG. 2. Left panel: Specular reflectivity curves from a 180-ML-thick Dy film at three different photon energies. The solid line through the data points and the subspectra show the results of fit analyses. The dotted lines represent the charge scattering contribution, and the dashed lines correspond to the magnetic satellite. Right panel: Optical parameters δ and β obtained from the fit analyses. The solid line represents β as obtained from the x-ray absorption spectroscopy (XAS) and scaled to the data; the dashed line shows its Kramers-Kronig transform.

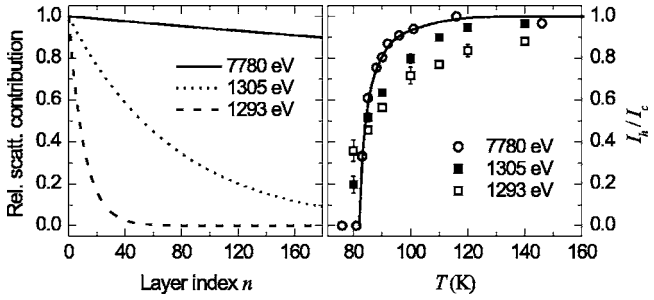

FIG. 3. Left panel: Relative scattering contribution as a function of the layer index n, where 0 denotes the surface layer. The data were calculated for different photon energies using the respective absorption coefficients and x-ray paths in the sample. Right panel: Scattering intensities upon heating normalized to the respective intensity on the cooling path: I_h/I_c.

temperature interval upon transition into the FM phase; it reappears when heating, but with a delay of $\approx$20 K (solid symbols). Notably, the (002-τ) intensity does not recover abruptly, but remains below the cooling-down curve up to $\approx$140 K, indicating a temperature-dependent growth of helical AFM domains. The even more gradual transition visible in the surface-sensitive measurement in Fig. 1(b) will be discussed below.

This growth occurs only along the surface normal as can be seen from the width of the magnetic diffraction peak as displayed in Fig. 1(c) for the directions perpendicular ($W_{q_\perp}$) and parallel ($W_{q_\parallel}$) to the film plane. When cooling, $W_{q_\perp}$ remains essentially constant down to $\approx$70 K; $W_{q_\perp} \approx 1.2 \times 10^{-2}$ Å^{-1} corresponds to 180 monolayers (ML) of Dy, i.e., the helical AFM structure extends through the whole film. Below $\approx$70 K, $W_{q_\perp}$ increases abruptly with the decay of the helical AFM order and—with increasing temperature—exhibits the same hysteresis as the intensity of (002-τ). In contrast, $W_{q_\parallel}$ is essentially constant in the studied temperature range, showing that the helical AFM domains develop in a laterally homogeneous way in the direction perpendicular to the film plane. An experiment with varying probing depth can hence be used to determine how this evolution occurs.

The variation of the probing depth across the Dy M_5 resonance can be seen in the specular reflectivity data taken in the range of the (000+τ) magnetic satellite from a 180-ML-thick Dy film as presented in the left panel of Fig. 2. Far away from the resonance, at 900 eV, the spectrum is dominated by charge scattering, the so-called Kiessig fringes, which can be described by interference between x rays reflected from the film's surface and its interface with the W substrate. The magnetic signal is visible only as a less pronounced minimum on a logarithmic scale. Near resonance (middle spectrum), the magnetic signal is strongly enhanced and a well pronounced magnetic peak can be seen. The Kiessig fringes are damped, because the penetration depth of the photons is now comparable to the film thickness. In the 1294 eV spectrum (upper) the Kiessig fringes are completely damped because there are no photons reflected from the interface—it can be easily seen that only a part of the sample volume is probed.

For the quantitative analysis, we describe the Kiessig fringes in the framework of the dynamical theory of reflectivity as demonstrated by Parratt.[13] The magnetic contribution to the data is described by the structure factor of a helical magnetic structure,[14]

$$F(q_\perp) \propto P e^{-1/2 q_\perp^2 \sigma_{\mathrm{rms}}^2} \sum_{n=1}^{N} e^{ind(q_\perp - \tau)}, \tag{1}$$

where P is a polarization factor, the Debye-Waller-type damping factor describes the roughness, N is the number of layers that contribute to the helix, $d=c/2$ denotes the layer spacing along the c direction, and τ is the magnetic modulation vector. The absorption and dispersion are accounted for by a complex wave vector $q_\perp = 4\pi/\lambda \sin(\sqrt{\Theta^2 - 2\delta + i2\beta})$, with Θ being the incidence and detection angle measured with respect to the sample surface, and $n = 1 - \delta + i\beta$ being the complex index of refraction. A superposition of the reflectivity and the magnetic diffraction signal describes all spectra in detail and the optical parameters, δ and β, can be obtained directly without further adjustable parameters. The resulting values for a set of energies are shown in the right panel of Fig. 2 together with β as obtained from the x-ray absorption spectrum and its Kramers-Kronig transform. The variation of the absorptive part, β, corresponds to an x-ray probing depth along the surface normal between 240 Å at 1305 eV and 17 Å and in the resonance maximum at 1292 eV at an angle of incidence $\Theta \approx 8.7°$.

By using a photon energy with small penetration depth, we can study the development of the AFM phase in the near-surface region. Figure 1(b) displays the integrated intensities of the (00τ) satellite as obtained at $h\nu = 1293$ eV where the effective x-ray probing depth is only $\approx$35 Å. Here, the intensity changes immediately, which shows that the helical AFM domain starts to grow near the surface. On the other hand, the full recovery of the helical AFM phase upon heating is even more delayed than at 7780 eV excluding a nucleation of the helical domain in the *topmost* surface layer.

For the quantitative analysis of the intensities we have to consider all effects that affect the intensity of the superstructure signal. Besides the temperature dependence of the domain size, which we are interested in, we also have to take into account the temperature dependence of the order parameter of the helical AFM structure and, less obvious, the temperature dependence of the magnetic period length. The latter leads to a change of the observation angle and thus a change of the x-ray path length through the sample. Since on

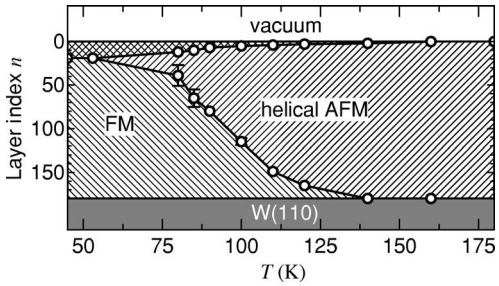

FIG. 4. Magnetic depth profile of a 180-ML-thick Dy film during the first-order phase transition from the FM to the helical AFM phase.

the cooling path the helical AFM structure is fully developed down to the AFM/FM phase transition this peak intensity can serve as a reference. The ratio of the intensities taken on the heating (I_h) and cooling path (I_c) thus contains only information about the fraction of AFM ordered layers in the *respective probed volume*—the AFM ordering parameter as well as the x-ray path length is eliminated in this ratio.

The relative scattering contribution and the intensity ratio I_h/I_c are shown in Fig. 3. Due to the small absorption at 7780 eV, all layers contribute with nearly the same strength to the scattered signal; I_h/I_c reflects the fraction of AFM ordered layers in the whole film. If the probing depth is limited by absorption, I_h/I_c is found to be larger close to the transition temperature and smaller for higher temperatures, which means that the AFM phase starts to develop *near* the surface faster than in the average of the film, but that the development in this region is not completed before the whole film is fully AFM ordered.

The complete depth profile, shown in Fig. 4, was derived from data recorded with various x-ray probing depths across the Dy M_5 resonance. The β values determined for the same film [Fig. 2(c)] were used to calculate the magnetic scattering amplitude of an individual layer n at depth d_n, which is reduced with respect to the topmost layer by $e^{-\mu d_n/\sin\theta}$.[15] The consistent analysis of temperature-dependent intensities leads to the following scenario: Upon cooling, the whole film orders helical AFM below $T_N \approx 179$ K. Below ≈ 125 K, a surface AFM structure with a longer period length develops in the topmost ≈ 19 layers. A similar trend is found in mean-field calculations of the free Ho surface.[16] Below ≈ 70 K, the film turns FM, except for the topmost layers that retain the surface AFM structure (crosshatched area). Upon heating, the helical AFM domain nucleates below this surface region and grows with increasing T towards the two interfaces. When reaching ≈ 140 K, it has developed across the whole film. A possible reason why the system studied here shows such a continuous transition in contrast to other Dy-film systems may be the symmetry of the low temperature phase, which may be stabilized by uniaxial strain from the bcc (110) substrate. That our film has two inequivalent boundaries while all other systems studied so far have symmetric boundaries may also play a role.

We point out that the present approach of exploiting the tunable x-ray probing depth across a resonance is not restricted to magnetic signals, and is also applicable to systems containing $3d$ transition elements, where at the $L_{2,3}$ resonances similarly strong absorption has been observed.[17] Such depth-dependent diffraction studies will be particularly interesting with focused x-ray beams providing additionally lateral resolution.[1]

Expert support by the staff members of BESSY and the ESRF is gratefully acknowledged, particularly the commitment of G. Grübel. The work was financially supported by the BMBF, project Nos. 05KS1KEE/8 and 03ZA6BC2, and the Sfb-290 (TPA06) of the DFG.

[1] P. G. Evans, E. D. Isaacs, G. Aeppli, Z. Cai, and B. Lai, Science **295**, 1042 (2002).
[2] H. Zabel, Physica B **198**, 156 (1994).
[3] G. P. Felcher, S. Adenwalla, V. O. De Haan, and A. A. Van Well, Nature (London) **377**, 409 (1995).
[4] H. Dosch, B. W. Batterman, and D. C. Wack, Phys. Rev. Lett. **56**, 1144 (1986).
[5] H. Dosch, Physica B **192**, 163 (1993).
[6] R. Günther, W. Donner, B. P. Toperverg, and H. Dosch, Phys. Rev. Lett. **81**, 116 (1998).
[7] M. B. Salamon, Shantanu Sinha, J. J. Rhyne, J. E. Cunningham, Rosse W. Erwin, Julie Borchers, and C. P. Flynn, Phys. Rev. Lett. **56**, 259 (1986).
[8] R. S. Beach, J. A. Borchers, A. Matheny, R. W. Erwin, M. B. Salamon, B. Everitt, K. Pettit, J. J. Rhyne, and C. P. Flynn, Phys. Rev. Lett. **70**, 3502 (1993).
[9] F. Tsui and C. P. Flynn, Phys. Rev. Lett. **71**, 1462 (1993).
[10] C. Schüßler-Langeheine, E. Weschke, Chandan Mazumdar, R. Meier, A. Yu. Grigoriev, G. Kaindl, C. Sutter, D. Abernathy, G. Grübel, and Manuel Richter, Phys. Rev. Lett. **84**, 5624 (2000).
[11] D. Gibbs, D. E. Moncton, K. L. D'Amico, J. Bohr, and B. H. Grier, Phys. Rev. Lett. **55**, 234 (1985).
[12] D. Gibbs, D. R. Harshman, E. D. Isaacs, D. B. McWhan, D. Mills, and C. Vettier, Phys. Rev. Lett. **61**, 1241 (1988).
[13] L. G. Parratt, Phys. Rev. **95**, 359 (1954).
[14] M. Blume and Doon Gibbs, Phys. Rev. B **37**, 1779 (1988).
[15] N. Bernhoeft, A. Hiess, S. Langridge, A. Stunault, D. Wermeille, C. Vettier, G. H. Lander, M. Huth, M. Jourdan, and H. Adrian, Phys. Rev. Lett. **81**, 3419 (1998).
[16] E. Weschke, H. Ott, E. Schierle, C. Schüßler-Langeheine, D. V. Vyalikh, G. Kaindl, V. Leiner, M. Ay, T. Schmitte, H. Zabel, and P. J. Jensen, Phys. Rev. Lett. **93**, 157204 (2004).
[17] J. B. Kortright and Sang-Koog Kim, Phys. Rev. B **62**, 12216 (2000).